

**REPORT DOCUMENTATION PAGE**

Form Approved OMB No. 0704-0188

Public reporting burden for this collection of information is estimated to average 1 hour per response, including the time for reviewing instructions, searching existing data sources, gathering and maintaining the data needed, and completing and reviewing the collection of information. Send comments regarding this burden estimate or any other aspect of this collection of information, including suggestions for reducing the burden, to Department of Defense, Washington Headquarters Services, Directorate for Information Operations and Reports (0704-0188), 1215 Jefferson Davis Highway, Suite 1204, Arlington, VA 22202-4302. Respondents should be aware that notwithstanding any other provision of law, no person shall be subject to any penalty for failing to comply with a collection of information if it does not display a currently valid OMB control number.

**PLEASE DO NOT RETURN YOUR FORM TO THE ABOVE ADDRESS.**

<b>1. REPORT DATE (DD-MM-YYYY)</b> 07-05-2010		<b>2. REPORT TYPE</b> Final Report		<b>3. DATES COVERED (From – To)</b> 28 September 2006 - 22-Jul-10	
<b>4. TITLE AND SUBTITLE</b>  Low Noise optical amplifiers			<b>5a. CONTRACT NUMBER</b> FA8655-06-1-3094		
			<b>5b. GRANT NUMBER</b>		
			<b>5c. PROGRAM ELEMENT NUMBER</b>		
<b>6. AUTHOR(S)</b>  Dr. Karsten Rottwitt			<b>5d. PROJECT NUMBER</b>		
			<b>5d. TASK NUMBER</b>		
			<b>5e. WORK UNIT NUMBER</b>		
<b>7. PERFORMING ORGANIZATION NAME(S) AND ADDRESS(ES)</b> Technical University of Denmark Building 345v Lyngby 2800 Denmark			<b>8. PERFORMING ORGANIZATION REPORT NUMBER</b>  N/A		
<b>9. SPONSORING/MONITORING AGENCY NAME(S) AND ADDRESS(ES)</b>  EOARD Unit 4515 BOX 14 APO AE 09421			<b>10. SPONSOR/MONITOR'S ACRONYM(S)</b>		
			<b>11. SPONSOR/MONITOR'S REPORT NUMBER(S)</b> Grant 06-3094		
<b>12. DISTRIBUTION/AVAILABILITY STATEMENT</b>  Approved for public release; distribution is unlimited.					
<b>13. SUPPLEMENTARY NOTES</b>					
<b>14. ABSTRACT</b> Optical amplifiers have been a topic of research over several decades. Throughout the early nineties research was focused on erbium doped fiber amplifiers, a technology which reached commercialization in the mid nineties and enabled the revolution within optical communication leading to long haul all optical communication links. Indirectly the erbium doped fiber amplifiers also enabled the progress that we witnessed within Raman amplifiers in the late nineties due to the development of suitable high power pump lasers enabled by rare earth doped fibers. Lately, research within optical amplifiers has been directed toward parametric optical amplifiers encouraged by a potential large gain bandwidth and low noise properties of these amplifiers. Currently erbium doped fiber amplifiers is the most mature optical amplifier technology and the safe choice, offering high gain and good noise properties from signal wavelengths from 1530 nm to 1610 nm. Raman amplifiers have proven superior noise properties when used as distributed amplifiers, compared to erbium doped fiber amplifiers. In addition Raman amplifiers, discrete as well as distributed offer wide bandwidth of operation since multiple pump lasers at different wavelengths may be combined to broaden the gain bandwidth. Finally, and maybe most important, the operation wavelength is solely determined by the wavelength of the pump laser, and Raman amplifiers from 1300 nm to 1610 nm have been demonstrated. Recent research has suggested parametric amplifiers as a promising alternative to erbium doped fiber amplifiers and Raman amplifiers offering low noise properties, wide bandwidth of operation and in addition wavelength conversion. Raman assisted parametric amplifiers have also been suggested.					
<b>15. SUBJECT TERMS</b> EOARD, Laser amplifiers, Raman laser materials, Fibre Lasers					
<b>16. SECURITY CLASSIFICATION OF:</b>			<b>17. LIMITATION OF ABSTRACT</b> UL	<b>18. NUMBER OF PAGES</b>  26	<b>19a. NAME OF RESPONSIBLE PERSON</b> A. GAVRIELIDES
<b>a. REPORT</b> UNCLAS	<b>b. ABSTRACT</b> UNCLAS	<b>c. THIS PAGE</b> UNCLAS			<b>19b. TELEPHONE NUMBER (Include area code)</b> +44 (0)1895 616205

## **Progress Report 4**

**Grant:**

**FA8655-06-1-3094**

## **Low Noise Optical Amplifiers**

**May 2010**

**Karsten Rottwitt**

**DTU Fotonik  
Department of Photonics Engineering,  
Technical University of Denmark**

**TABLE OF CONTENTS**

1. Introduction.....3

2. Influence of variations of group velocity dispersion.....3

3. Other results..... 4

    3.1 Semi-analytical model.....4

    3.2 Nonlinear Stokes analysis.....4

4. Ongoing activities.....5

5. Conclusion.....6

    5.1 Publications from the project.....6

6. Future work.....7

    People

    Activities

Enclosures: .....8

Submitted and “to be submitted” publications from the relevant period

## 1 Introduction

In the past term we have continued our effort towards understanding amplification in single as well as double wavelength pumped parametric amplifiers when these are operated in depletion. Two applications that we have in mind are wavelength conversion and signal regeneration. In addition, we have also looked into the possibility of using the fourth order derivative of the propagation constant  $\beta_4$  to obtain phase matching at large wavelength shifts from the wavelength of the pump.

Our effort has been mainly theoretical however, we are in the process of designing and putting together a new phase sensitive amplifier. The following sections provide a status report on our results. In Section 2 results on investigations of fluctuations of the group velocity dispersion on the gain spectrum of a parametric fiber amplifier are described. This effort has resulted in a publication at the forthcoming OSA Topical meeting on nonlinear photonics. The manuscript is included in enclosure 1. In Section 3 theoretical results on depletion and nonlinear Stokes analysis is described. We are currently putting these results together in two publications that we expect to submit to Optics Express within the coming months. Both papers at their current state are included to this report as enclosures 2 and 3. Finally, Section 4, describes our current effort.

Section 5 concludes this status report.

## 2 Influence of variations of group velocity dispersion (enclosure 1)

The spectral shape of the gain of a parametric process in an optical fiber depends on the group velocity dispersion of the optical fiber, the initial pump and signal powers, and the wavelength of the pump. These parameters can be chosen to create a balance between the second and fourth order group velocity dispersion terms, such that the gain spectrum consists of two gain regions on each side of the wavelength of the pump, see Fig 1, which show the gain spectrum resulting from a 350 m long fiber pumped by 1 Watt. Three cases are considered corresponding to three different pump wavelengths. The second gain region, i.e. the gain region furthest away from the pump, is of interest for broad wavelength conversion or when working outside the conventional C and L bands. For narrow peaks ( $< 1$  nm) it also enables applications such as a narrow-band filter with gain or as a gain medium in fiber lasers with tuneable wavelength. On the other hand if the gain spectrum is broad ( $> 10$  nm), it could be used for amplification in WDM systems, while still avoiding four wave mixing between the channels.

The numerical simulations shown in Fig.1, illustrate how random fluctuations, according to a normal distribution, of the group velocity dispersion along the fiber strongly influence both gain peaks in the gain spectrum and especially the gain peak occurring furthest away from the pump wavelength. The considered fluctuations in the group velocity dispersion, are similar to those existing in state of the art highly nonlinear optical fibers. From the figure it is obvious that the spectral gain profile is strongly modified and the second gain peak disappears.

Further details/discussions on this topic are found in enclosure 1, which is a copy of the manuscript accepted for presentation at the forthcoming OSA Topical Meeting on Nonlinear Photonics, to be held in Karlsruhe, Germany, June 21-24, 2010..

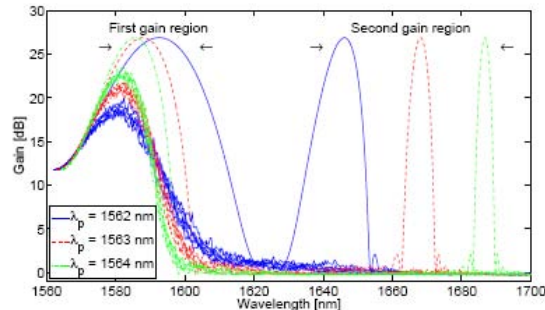


**Figure 1:** Gain versus signal wavelength for three pump wavelengths. The launched signal and idler power is 0.1 mW. The lines reaching 25 dB of gain are with no variations in group velocity dispersion, whereas the other lines are obtained with realistic variations in group velocity dispersion.

### 3 Other results

In addition to the work on impact do to fluctuations in group velocity dispersion we have continued our effort on theoretical modelling of the parametric fiber amplifiers. Our most recent results are described below.

#### 3.1 Semi-analytical model (enclosure 2):

One important application of the parametric amplifier is when it is operated in depletion, since this has use in communication systems as regenerating amplifiers or as wavelength converters.

We have derived a semi-analytic model of the dual pumped parametric amplifier that includes pump depletion. The analytic solution is found by using Jacobian Elliptic functions. These functions are not easy to use however, with a few but reasonable approximations we have obtained some much simpler and useful expressions. We have used this model to show that wide and flat gain is achievable with the dual pumped FOPA. In addition, the theoretical modelling shows that a phase mismatch which equals the product of the nonlinear strength times the signal power leads to complete power conversion.

Further details and discussions are found in enclosure 2, which is a version of a manuscript that we are currently writing, which describes the semi-analytical model of the depleted parametric amplifier. We plan on submitting the manuscript to Optics Express within May.

#### 3.2 Nonlinear Stokes analysis (enclosure 3)

To get further into a detailed description of noise issues we have studied the dynamics of the four-wave mixing (FWM) equations using a Stokes like parametrization of the Fields. The parametrization is chosen so as to use symmetry of the Gauge invariance of the FWM equations. This has enabled us to reduce the dynamics of FWM to the

one-dimensional intersection between the phase-plane of the conserved Hamiltonian and the closed two-dimensional iso-power surface in a three-dimensional phase-space. In this way both the phases and amplitudes of the mixing fields can be visualized simultaneously giving a complete overview of the FWM dynamics. Further details are described in enclosure 3, which is a current version of manuscript that we are planning on submitting to Optics Express within the coming months.

The analysis is advantageous since non-degenerate FWM as in two pump optical parametric amplification is strongly phase dependent. The analysis also visualizes the effect of noise as noise will manifest itself as a perturbation of the iso-power surface which might be useful for analysis of the noise limits for depleted parametric amplifiers.

#### **4. Ongoing activities**

The activities described above are all completed to a level where results are close to being submitted for publication or even published. In addition to these activities we also have activities that we are currently working on, but where we at present time do not have results that may be published.

Most important are our activities related to systems demonstrations of phase sensitive amplifications. These activities have been funded by the Danish technical research council but have been seeded by this current project. We have only just started the project and have hired a post doc and one ph.d. student. However, at this point in time we have no results.

In addition to the program on phase sensitive amplifiers we have initiated a master student project entitled: "Pulse-deformation in parametric amplifier" Within the project a parametric amplifier will be used as the amplifier in a fiber ring laser, and formation of short pulses will be studied. The program has just been initiated and at this point in time the project has not given any results.

Finally, in collaboration with Colin Mc.Kinstrie, Alcatel-Lucent, NJ, USA, we have been working on Self Seeded Four wave mixing. This is the process where strong pumps interact during propagation and create two additional self-seeded pumps. The two strong pumps interact in degenerate parametric amplification to create two sidebands. When these are created, all four also interacts in a non-degenerate parametric process. The evolution of these four pumps is investigated with focus on creating four equal pumps suited for multicasting.

We have performed a theoretical study of this process and are currently discussing the results.

## 5. Conclusion

In the term covered by this report we have focussed partly on the impact of fluctuations along the length of the fiber through which amplification is achieved in the parametric amplifier and partly on theoretical modeling.

In parametric amplifiers there exists two gain peaks one relatively close to the pump, tens of nanometers from the pump, and one further away, up to hundreds of nanometers from the pump. The second peak is very interesting for the purpose of wavelength conversion. However, we have demonstrated that due to variations in the group velocity dispersion, similar to those existing in state of the art highly nonlinear optical fibers, the spectral gain profile is strongly modified and the second gain peak disappears.

Regarding the theoretical modelling we have shown a semi-analytical model which is capable of predicting gain of single as well as dual pumped parametric amplifiers when these are operated in depletion. From the theoretical modelling it is shown that a phase mismatch which equals the product of the nonlinear strength times the signal power leads to complete power conversion.

### 5.1 Publications from the project

L. S. Rishøj and K. Rottwitt, "Influence of Variations of the GVD on Wavelength Conversion at Second Gain Region of a Parametric Process," Accepted for presentation at Nonlinear Photonics 2010

K. Rottwitt, J. R. Ott, H. Steffensen, S. Ramachandran, "Spontaneous emission from saturated parametric amplifiers," ICTON'09 Azores, Portugal, 2009

C. Peucheret, M. Lorenzen, J. Seoane, D. Noordegraaf, C.V. Nielsen, L. Grüner-Nielsen and K. Rottwitt, "Amplitude regeneration of RZ-DPSK signals in single pump fiber optics parametric amplifiers," IEE photonics Technol. Letters, Vol. 21, No. 13, p 872, 2009

M. R. Lorenzen, D. Noordegraaf, C.V. Nielsen, O. Odgaard, L. Grüner-Nielsen and K. Rottwitt, "Suppression of Brillouin scattering in fibre-optical parametric amplifier by applying temperature control and phase modulation," Electron Lett. Vol. 45, No. 2, p 125, 2009

M. R. Lorenzen, D. Noordegraaf, C.V. Nielsen, O. Odgaard, L. Grüner-Nielsen and K. Rottwitt, "Brillouin Suppression in a fiber optical parametric amplifier by combining temperature distribution and phase modulation," in proc. OFC'08, paper OML1, 2008

C. Peucheret, M. Lorenzen, J. Seoane, D. Noordegraaf, C.V. Nielsen, L. Grüner-Nielsen and K. Rottwitt, "Dynamic range enhancement and amplitude regeneration in single pump fibre optic parametric amplifiers using DPSK modulation," in proc ECOC'08, Brussels

K. Rottwitt, M. Lorenzen, D. Noordegraaf and C. Peucheret, "Gain characteristics of a saturated fiber optic parametric amplifier," in Proc. ICTON'08 Athens Greece, paper Mo.D1.1

J.M. Chavez Boggio, J. R. Windmiller, M. Knutzen, R.Jiang, C. Bres, N. Alic, B. Stossel, K. Rottwitt and S. Radic, "730 nm optical parametric conversion from near to short wave infrared band," Optics Express, vol. 16, No. 8, p 5435, Apr. 2008

J.M. Chavez Boggio, M. Knutzen, R.Jiang, C. Bres, N. Alic, J. R. Windmiller, B. Stossel, K. Rottwitt and S. Radic, "730 nm optical parametric conversion from near to short wave infrared band," Optics Express, vol. 16, No. 8, p 5435, Apr. 2008

D. Noordegraaf, M. Lorenzen, C.V. Nielsen and K. Rottwitt, "Brillouin scattering in fiber optical parametric amplifiers," ICTON'07, paper We.A1.5

## **6. Future work**

### ***People:***

Within the period of this report, Toke Lund Hansen has started as a post doc. supervised by Karsten Rottwitt. Toke will be performing mainly experimental research on phase sensitive amplification. In addition, a new ph.d. student Valentina Christofioi has just started studies toward a PhD degree on parametric fiber amplifiers. In addition, activities within the systems group at DTU Fotonik, has intensified through two new ph.d positions within parametric amplifiers, one partly funded through a research program on phase sensitive amplifiers funded through the Danish technical research council and the other funded by a so-called internationalization program.

### ***Activities:***

As indicated in the above DTU Fotonik now has significant activities on using parametric processes in optical fibers. This includes fundamental studies on noise issues, fibers for parametric devices and also system aspects of parametric amplifiers and more specifically phase sensitive amplifiers and amplification of very short pulses (few hundred femto second in pulse width). In addition, DTU Fotonik also have initiated collaboration external partners in relation to parametric amplifiers, this include collaboration with OFS Fitel Denmark, with Prof. Stojan Radic, University of San Diego and Prof. Siddharth Ramachandran Boston University.

## **ACKNOWLEDGEMENTS**

We would like to acknowledge OFS Fitel Denmark for providing the HNL-DSF.

## **Enclosures**

*Publications resulted from the project (in the period of this report)*

Accpeted:

[1] L. S. Rishøj and K. Rottwitt, "Influence of Variations of the GVD on Wavelength Conversion at Second Gain Region of a Parametric Process," Accepted for presentation at Nonlinear Photonics 2010

In Preparation:

[2] H. Steffensen, et al, "Full and Semin-Analytic Two-Pump Parametric Amplification with Pump Depletion" to be submitted

[3] J.R. Ott, et. Al., "Geometric Interactions of Four Wave Mixing" to be submitted

# Influence of Variations of the GVD on Wavelength Conversion at Second Gain Region of a Parametric Process

Lars S. Rishøj and Karsten Rottwitt

DTU Fotonik, Department of Photonics Engineering, Technical University of Denmark,  
Oersteds Plads 343, DK-2800 Kgs. Lyngby, Denmark  
iris@fotonik.dtu.dk, karo@fotonik.dtu.dk

**Abstract:** Impact on the second gain region in a parametric process, caused by random variations of the group velocity dispersion along the fiber is demonstrated. The model includes both pump depletion and fiber loss.

© 2010 Optical Society of America

**OCIS codes:** (190.4370) Nonlinear optics, fibers; (190.4410) Nonlinear optics, parametric processes.

## 1. Introduction

The shape of the gain spectrum depends on the group velocity dispersion (GVD) of the fiber, the initial pump and signal powers, and the wavelength of the pump. These parameters can be chosen to create a balance between the second and fourth order dispersion terms, such that the gain spectrum consists of two gain regions on each side of the wavelength of the pump. Through simulations this paper focuses on the gain peak occurring furthest away from the pump wavelength, referred to as the second gain region. This gain region is of interest for broad wavelength conversion or when working outside the conventional C and L bands. For narrow peaks ( $< 1$  nm) it also enables applications such as a narrow-band filter with gain or as a gain medium in fiber lasers with tunable wavelength. On the other hand if the gain spectrum is broad ( $> 10$  nm), it could be used for amplification in WDM systems and hereby avoiding FWM phase matching between the channels. Unlike previous publications within this field, this model also accounts for pump depletion and fiber loss. The former of these have previously been neglected, by arguing that pump depletion rarely occurs in experiments. However, it is important when trying to obtain large power transfer during wavelength conversion. Also, recently depleted parametric amplifiers have been used for signal regeneration [1].

## 2. Description of the Model

A crucial criterion for the parametric process is to achieve phase matching between the interacting waves, i.e. between the signal, idler, and pump. In the case of a degenerated pump, the parametric process depends on the linear phase mismatch [2]. By Taylor expanding this around the frequency of the pump, one yields

$$\Delta\beta = 2 \sum_{m=1}^{\infty} \frac{\beta_{2m,p}}{(2m)!} (\omega_s - \omega_p)^{2m}. \quad (1)$$

From this it is seen that any variations of the GVD along the fiber will influence the gain spectrum in an unknown manner. The fiber parameters used for the simulations are for a highly nonlinear dispersion shifted fiber (HNLF). This fiber has a nonlinear coefficient of  $\gamma = 11.5 \text{ W}^{-1}\text{m}^{-1}$  and a loss of  $\alpha = 0.74 \text{ dB/km}$ , these are assumed to be independent of wavelength. Furthermore, the fiber has a zero dispersion wavelength of  $\lambda_0 = 1559.5 \text{ nm}$  and a slope at this wavelength equal to  $S = 0.015 \text{ ps}/(\text{nm}^2\text{km})$ . For this HNLF  $\beta_{4,p} > 0$ , thus by ensuring that  $\beta_{2,p} < 0$ , it is possible to obtain gain by balancing the two first terms of Eq. (1). Simulations have shown that if no variation of the GVD is included it is possible to obtain wavelength conversion over more than 300 nm by using merely 1 W of pump power, by selecting the wavelength of the pump accordingly.

Variations of the GVD in fibers are caused by changes in the core radius and the refractive index along the fiber. The latter contribution has been neglected in the model, furthermore the effect these core changes has on the effective area and thus the nonlinear coefficient has also been neglected. The relative change in the core diameter is for recent fabricated HNLF reported to be around  $\pm 0.03 \%$  over 500 m [3]. Using a full vectorial mode solver it was found that a change of  $0.03 \%$  in the core diameter of the HNLF described above, leads to a change in the GVD of  $0.03 \text{ ps}/(\text{nm} \cdot \text{km})$  at  $\lambda_0$ ; this corresponds to a change in the zero dispersion wavelength of 2 nm. Furthermore, the simulations with the mode solver verified that it is only a minor assumption to model the variations of the GVD as vertical translations of the entire GVD curve, hence this is utilized in the following simulations. The GVD along the fiber is modeled by adding variations according to a stochastic variable following a normal distribution, this is similar to the method used in [4, 5]. The distance between these random generated points is denoted  $L_{var}$  and the GVD between these points are approximated to be linear. The symbol used for the standard deviation is  $\sigma$ .

### 3. Simulation Results

It is found that the pump is fully depleted when the pump wavelength is  $\lambda_p = 1564$  nm and no variations of the GVD are included, if the signal wavelength is  $\lambda_s = 1554$  nm and the fiber length is  $L_{opt} = 347$  m, hence working in the first gain region. This situation is referred to as ideal and has been used for normalization. Since a stochastic variable is included, the simulations have been carried out 1000 times. It was seen that the distribution for any parameters follows an exponential behavior, which peaks at a normalized idler power of one. However, the spread becomes narrower as  $L_{var}$  and  $\sigma$  decrease, these results have not been included here. In Fig. 1 it is seen that the minimum power of the idler increases as  $L_{var}$  and  $\sigma$  decrease. This indicates that even in the worst case scenario a significant conversion efficiency is obtained, if the variations are on the order of or shorter than a few meters.

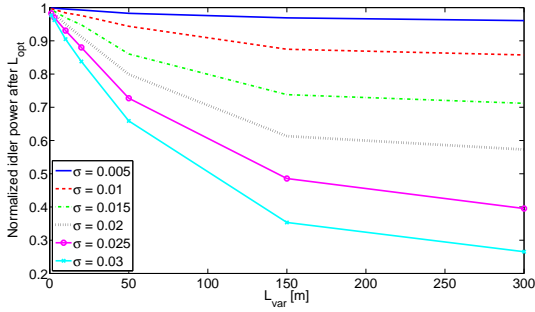


Fig. 1. The parameters for the simulation are  $\lambda_s = 1554$  nm and  $\lambda_p = 1564$  nm. The minimum normalized idler power after the optimal length of propagation. The bottom 10% of the simulations have been removed in order not to obscure the tendencies. The legend indicates the standard deviation of the normal distribution in units of ps/(nm · km).

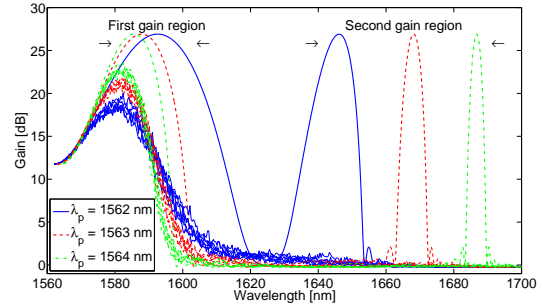


Fig. 2. The gain spectrum for different wavelengths and with a fiber length of  $L = 350$  m. The parameters are  $P_{p,i} = 1$  W and  $P_{s,i} = 0.1$  mW. The lines reaching gain over 25 dB are with no variations of the GVD, whereas the remaining lines are for variations where  $\sigma = 0.01$  ps/(nm · km) and  $L_{var} = 1$  m.

Next, a similar analysis is performed for the gain region that occurs further away from the wavelength of the pump, also referred to as the second gain region. In these simulations  $\lambda_s$  and  $L$  was chosen such that full depletion of the pump is obtained, if no variations of the GVD are included. It was seen that hardly any idler power is generated. In general the tendency is that as  $L_{var}$  decreases or  $\sigma$  increases the distribution becomes narrower and closer to zero. Also the spread of the idler powers becomes larger as  $\lambda_p$  becomes smaller, these results are not included here. Fig. 2 shows the gain spectra for three different wavelengths of the pump, both with no variations of the GVD and with six different random variations, the initial signal power is set to  $P_{s,0} = 0.1$  mW. It is seen that the gain spectrum is seriously degraded by the introduction of variations, especially it is noticeable that the second gain region is basically non-exciting for all of the three wavelengths of the pump. However, a certain amount of gain is still obtained for wavelengths close to the wavelength of the pump. This is not obvious by observing the Taylor expansion of the phase matching condition, since as  $\lambda_p$  gets closer to  $\lambda_0$  the relative change in  $\beta_{2,p}$  due to the same sized variations gets larger, which would increase the impact of the variations. On the other hand the gain peak is moved such that  $|\omega_p - \omega_s|$  becomes smaller and also the gain peak becomes wider, which both reduce the impact from the variations. A solution would be to increase the pump power and thereby reduce the needed fiber length, and thus in effect reduce the impact of the variations of the GVD.

### 4. Conclusion

It was shown that introducing variations of the GVD of a magnitude similar to those expected in modern HNLFF, the parametric process was influenced to an extent such that the gain peak, caused by the balancing of the terms involving  $\beta_{2,p}$  and  $\beta_{4,p}$  in the phase matching condition, would cease to exist.

### References

- [1] C. Peucheret, M. Lorenzen, J. Seoane, D. Noordegraaf, C. V. Nielsen, K. Rottwitz, and L. Grüner-Nielsen, "Dynamic range enhancement and amplitude regeneration in single pump fibre optic parametric amplifiers using dpsk modulation," *ECOC*, 2008.
- [2] J. Hansryd, P. Andrekson, M. Westlund, J. Li, and P.-O. Hedekvist, "Fiber-based optical parametric amplifiers and their applications," *IEEE Journal of Selected Topics in Quantum Electronics*, vol. 8, no. 3, pp. 506–520, 2002.
- [3] M. Hirano, T. Nakanishi, T. Okuno, and M. Onishi, "Silica-based highly nonlinear fibers and their application," *IEEE Journal of Selected Topics in Quantum Electronics*, vol. 15, no. 1, pp. 103–113, 2009.
- [4] F. Yaman, Q. Lin, S. Radic, and G. Agrawal, "Impact of dispersion fluctuations on dual-pump fiber-optic parametric amplifiers," *IEEE Photonics Technology Letters*, vol. 16, no. 5, pp. 1292–1294, 2004.
- [5] M. Karlsson, "Four-wave mixing in fibers with randomly varying zero-dispersion wavelength," *Journal of the Optical Society of America B (Optical Physics)*, vol. 15, no. 8, pp. 2269–2275, 1998.

# Full and Semi-Analytic Two-Pump Parametric Amplification with Pump Depletion

H. Steffensen,<sup>1,\*</sup> J. R. Ott,<sup>1</sup> K. Rottwitt,<sup>1</sup> and C. J. McKinstrie,<sup>2</sup>

<sup>1</sup> Department of Photonics Engineering, Technical University of Denmark, 2800 Lyngby, Denmark

<sup>2</sup> Bell Laboratories, Alcatel-Lucent, Holmdel, New Jersey 07733

\*[hste@fotonik.dtu.dk](mailto:hste@fotonik.dtu.dk)

**Abstract:** This paper solves the four coupled equations describing non-degenerate FWM, with the focus on amplifying a signal in a fiber optical parametric amplifier (FOPA). Based on the full analytic solution, a simple approximate solution describing the gain is developed. The advantage of this new approximation is that it includes the depletion of the pumps, which is lacking in the usual quasi-linearized approximation. Using this approximate solution we demonstrate the possibility of achieving a flat gain over 87 nm centered at 1560.5 nm.

© 2010 Optical Society of America

OCIS codes: (000.0000) General.

---

## References and links

1. S. Radic, C. J. McKinstrie, R. M. Jopson, J. C. Centanni, and A. R. Chraplyvy, "All-optical regeneration in one- and two-pump parametric amplifiers using highly nonlinear optical fiber," **15**, 957–960 (2003).
2. M. Matsumoto, "Regeneration of rz-dpsk signals by fiber-based all-optical regenerators," **17**, 1055–1057 (2005).
3. C. Peucheret, M. Lorenzen, J. Seoane, D. Noordegraaf, C. V. Nielsen, K. Rottwitt, and L. Gruner-Nielsen, "Amplitude regeneration of rz-dpsk signals in single-pump fiber-optic parametric amplifiers," **21**, 872–874 (2009).
4. K. Inoue, "Suppression of level fluctuation without extinction ratio degradation based on output saturation in higher order optical parametric interaction in fiber," **13**, 338–340 (2001).
5. M. Matsumoto, "Performance improvement of phase-shift-keying signal transmission by means of optical limiters using four-wave mixing in fibers," *J. Lightwave Technol.* **23**, 2696–2701 (2005).
6. M. E. Marhic, *Fiber Optical Parametric Amplifiers, Oscillators and Related Devices* (Cambridge University Press, New York, NY, USA, 2007).
7. C. J. McKinstrie, X. D. Cao, and J. S. Li, "Nonlinear detuning of four-wave interactions," *J. Opt. Soc. Am. B* **10**, 1856–1869 (1993).
8. G. Cappelline and S. Trillo, "Third-order three-wave mixing in single-mode fibers: exact solutions and spatial instability effects," *J. Opt. Soc. Am. B* **8**, 824–838 (1990).
9. P. Kylemark, H. Sunnerud, M. Karlsson, and P. A. Andrekson, "Semi-analytic saturation theory of fiber optical parametric amplifiers," *J. Lightwave Technol.* **24**, 3471–3479 (2006).
10. J. M. Chávez Boggio, P. Dainese, F. Karlsson, and H. L. Fragnito, "Broad-band 88% efficient two-pump fiber optical parametric amplifier," **15**, 1528–1530 (2003).
11. C. J. McKinstrie and G. G. Luther, "Solitary-wave solutions of the generalised three-wave and four-wave equations," *Phys. Rev. A* **127**, 14–18 (1988).
12. G. P. Agrawal, *Nonlinear Fiber Optics* (Academic Press, 2007), 4th ed.
13. K. Inoue, "Polarization effect on four-wave mixing efficiency in a single-mode fiber," *IEEE J. Quantum Electron.* **28**, 883–894 (1992).
14. C. J. McKinstrie, H. Kogelnik, R. M. Jopson, S. Radic, and A. V. Kanaev, "Four-wave mixing in fibers with random birefringence," *Opt. Express* **12**, 2033–2055 (2004).
15. J. Hansryd, P. A. Andrekson, M. Westlund, J. Li, and P.-O. Hedekvist, "Fiber-based optical parametric amplifiers and their applications," *IEEE J. Sel. Top. in Quantum Electron.* **8**, 506–520 (2002).

16. J. M. Manley and H. E. Rowe, "Some general properties of nonlinear elements - part 1. general energy relations," Proc. IRE **44**, 904–913 (1956).
  17. M. T. Weiss, "Quantum derivation of energy relations analogous to those for nonlinear reactances," Proc. IRE **45**, 1012–1013 (1957).
  18. P. F. Byrd and M. D. Friedman, *Handbook of elliptic integrals for engineers and physicists* (Springer, 1954).
  19. M. Hirano, T. Nakanishi, T. Okuno, and M. Onishi, "Silica-based highly nonlinear fibers and their application," IEEE J. Sel. Top. in Quantum Electron. **15**, 103–113 (2009).
- 

## 1. Introduction

Parametric amplifiers have shown promising features in a wide variety of applications beside just amplification of signals. It has potential as optical regenerators [1, 2, 3] based on either one or two pumps, to suppress level fluctuation [4], and also as noise limiters, for instance to limit amplified spontaneous emission (ASE) noise or to reduce nonlinear phase noise [5].

Dual pumped Parametric amplifiers show potential application as amplifiers with a very wide bandwidth of operation and a flat gain throughout the bandwidth window of operation [6]. However, it is more complicated to predict their performance analytically since four coupled wave equations needs to be solved. In this work we demonstrate the existing analytical solutions using elliptic Jacobian functions [7, 8], and based on these we show that simple approximations exist that enable predictions of depletion performance of double wavelength pumped parametric amplifiers.

Previously Kylemark et al. [9] have derived a useful approximation for a single pump FOPA operated at the total conversion phase mismatch. This paper uses a similar approach on the dual pumped FOPA and extends it to the full range of phase mismatch. We use the approximation on a specific example where it is shown that a flat and wide gain is achieved with pumps placed symmetric around the zero dispersion wavelength (ZDW). A flat gain over 25 nm have previously been experimentally realized, [10], but in this paper we predict a flat broadband gain over 87 nm.

## 2. Theory

In general we consider an electric field consisting of four CW waves, at frequencies  $\omega_1$  through  $\omega_4$ . In non-degenerate FWM, the four distinct waves interact with each other under the condition that  $\omega_1 + \omega_4 = \omega_2 + \omega_3$ . Two of these, number 2 and 3, are in this paper used as pumps, while 1 is a signal, also denoted  $s$ , that is to be amplified, and 4 is the idler,  $i$ , that arise when the signal is amplified. The envelope of the field is, for parallel pumps and signal, governed by [11, 12]

$$\frac{dA_1}{dz} = i\beta_1 A_1 + i\gamma \{ [|A_1|^2 + 2(|A_2|^2 + |A_3|^2 + |A_4|^2)] A_1 + 2A_2 A_3 A_4^* \} \quad (1a)$$

$$\frac{dA_2}{dz} = i\beta_2 A_2 + i\gamma \{ [|A_2|^2 + 2(|A_1|^2 + |A_3|^2 + |A_4|^2)] A_2 + 2A_1 A_3^* A_4 \} \quad (1b)$$

$$\frac{dA_3}{dz} = i\beta_3 A_3 + i\gamma \{ [|A_3|^2 + 2(|A_1|^2 + |A_2|^2 + |A_4|^2)] A_3 + 2A_1 A_2^* A_4 \} \quad (1c)$$

$$\frac{dA_4}{dz} = i\beta_4 A_4 + i\gamma \{ [|A_4|^2 + 2(|A_1|^2 + |A_2|^2 + |A_3|^2)] A_4 + 2A_1^* A_2 A_3 \}, \quad (1d)$$

where  $\gamma$  is the nonlinear strength and  $\beta_\alpha$  is the wave number, index  $\alpha$  may be either 1, 2, 3 or 4. In the case of perpendicular pumps and sidebands, the factor of 2 in the coupling term should be changed to a 1 [13, 14]. The most common method of solving Eq. (1) is by assuming that the pump powers remain much greater than the signal and idler power at all times and that the

power loss of the pumps is negligible [15]. This will quasi-linearize the differential equations and for pumps with identical power,  $P_p$ , result in

$$P_s(z) = P_s(0) \left\{ 1 + \left[ \frac{2\gamma P_p}{g} \sinh(gz) \right]^2 \right\} \quad (2)$$

$$P_i(z) = P_s(0) \left[ \frac{2\gamma P_p}{g} \sinh(gz) \right]^2 \quad (3)$$

where  $g^2 = (2\gamma P_p)^2 - (\kappa/2)^2$  and  $\kappa = 2\gamma P_p + \Delta\beta$ .  $\Delta\beta$  is the phase mismatch given as  $\Delta\beta = \beta_1 - \beta_2 - \beta_3 + \beta_4$ , and since  $P_p$  is the pump power in each pump and these are assumed identical, the expression resembles the expression known from single pumped parametric amplifiers [15]. Based on this solution, the highest growing gain,  $G(z) = P_s(z)/P_s(0)$ , is obtained with  $\kappa = 0$ , thus requiring that  $\Delta\beta = -2\gamma P_p$ . Generally, gain exist when  $-6\gamma P_p < \Delta\beta < 2\gamma P_p$ . The problem with this solution is that it does not account for either pump depletion or nonlinear detuning, which is caused by the change in relative phase as the power is transferred.

Instead of rewriting the complex amplitude  $A$  in Eq. (1) into the real variables, power  $P$  and phase  $\phi$ , as  $A_\alpha = \sqrt{P_\alpha} \exp(i\phi_\alpha)$ , the differential equations are instead written as

$$\frac{dP_\alpha}{dz} = s_\alpha 4\gamma \sqrt{\prod_\beta P_\beta} \sin(\theta) \quad (4)$$

$$\frac{d\phi_\alpha}{dz} = \beta_\alpha + \gamma(2 \sum_\beta P_\beta - P_\alpha) + 2\gamma \frac{\sqrt{\prod_\beta P_\beta}}{P_\alpha} \cos(\theta) \quad (5)$$

where  $\theta = \phi_1 + \phi_4 - \phi_2 - \phi_3$  and  $s_\alpha = \frac{d\theta}{d\phi_\alpha}$ . It is seen that only the relative phase,  $\theta$ , and not the individual phases, is important, thus the phase equations can be reduced to one single differential equation. As seen from Eq. (4), this relative phase is important as it shows to which direction the power flows, if the relative phase is positive, the power is transferred from the pumps to the signal and idler, if the relative phase is negative, the opposite happens. As power is transferred from the pumps to the signal and idler, nonlinear detuning occurs which reduces the coupling. At some point the relative phase can be changed so much that the power flow is reversed and the power begins to couple back to the pumps.

Because the parametric process is symmetric, the signal and the idler have the same increase in power, while the pumps have the same decrease, also written as  $d_z(P_s - P_i) = 0$  and  $d_z(P_2 - P_3) = 0$ . Finally, the process is power conserving thus  $\sum_\alpha P_\alpha(z) = P_{total}$ . Based on this, all powers are related to each other, and can thus be described by only one variable according to the Manley-Rowe relations [16, 17]. This variable,  $F$ , is chosen to be the power of the idler which is assumed zero at  $z = 0$ , i.e.

$$P_1 = P_s + F \quad (6a)$$

$$P_2 = P_3 = P_p - F \quad (6b)$$

$$P_4 = F, \quad (6c)$$

where  $P_s$  is the input power of the signal, and  $P_p$  is the input power for each of the two pumps. With this notation, the gain of the signal is found as

$$G(z) = \frac{P_s(z)}{P_s(0)} = 1 + \frac{F(z)}{P_s}. \quad (7)$$

From Eq. (6), two governing differential equations can be set up for the power,  $F$ , and the phase,  $\theta$ ,

$$\frac{dF}{dz} = 4\gamma(P_p - F)\sqrt{F(P_s + F)}\sin(\theta) \quad (8)$$

$$\frac{d\theta}{dz} = 2\gamma \left[ (P_p - F) \left( \sqrt{\frac{F}{P_s + F}} + \sqrt{\frac{P_s + F}{F}} \right) - 2\sqrt{F(P_s + F)} \right] \cos(\theta) + \gamma\delta - 4\gamma F \quad (9)$$

where

$$\delta = \frac{\Delta\beta}{\gamma} + 2P_p - P_s, \quad (10)$$

This effective phase mismatch also includes the signal power, which in the quasi-linearized case is omitted due to the assumptions made. The two differential equations have the Hamiltonian

$$H = 4\gamma(P_p - F)\sqrt{F(P_s + F)}\cos(\theta) + \gamma(\delta - 2F)F. \quad (11)$$

This has been found by using a qualified guess and knowing it has to fulfill Hamilton's equations as given by

$$\frac{dF}{dz} = -\frac{\partial H}{\partial \theta}, \quad \frac{d\theta}{dz} = \frac{\partial H}{\partial F}. \quad (12)$$

The first term on the RHS of Eq. (11) is due to FWM, while the second contains the linear and nonlinear phase terms. Because the Hamiltonian is independent of  $z$ , it is constant. It is therefore used to reduce the problem to one variable. Since  $F$  is initially zero, the value of the Hamiltonian is also zero. With this the phase,  $\theta$ , can be determined as

$$\cos(\theta) = \frac{-(\delta - 2F)F}{4(P_p - F)\sqrt{F(P_s + F)}}. \quad (13)$$

From Eq. (8) a potential equation may be obtained for  $F$ , by squaring the equation and inserting the expression for  $\theta$ , resulting in

$$\left(\frac{dF}{dz}\right)^2 = \gamma^2 \left[ 16(P_p - F)^2 F(P_s + F) - (\delta - 2F)^2 F^2 \right] \quad (14)$$

For any given value of the wave-number mismatch, this can be written as

$$\left(\frac{dF}{dz}\right)^2 = 12\gamma^2 F(f_1 - F)(f_2 - F)(F - f_3) \quad (15)$$

where  $f_j$ , ( $j \in (1, 2, 3)$ ) are the roots of the polynomial and  $f_1 \geq f_2 > F(0) > f_3$ . The ordering of these roots are important because it affects the structure of the solution. The solution for  $F$  will be bounded by the roots of the potential equation. The lower boundary is zero, and the upper boundary is the root  $f_2$ . The value of this root will thus be the maximum value of the added power to both the signal and the idler. The differential equation can be solved using Jacobian Elliptic Functions [18], the solution is:

$$F(z) = \frac{f_3 f_2 \operatorname{sn}^2 \left[ \gamma z \sqrt{3f_1(f_2 - f_3)}, m \right]}{-f_2 + f_3 + f_2 \operatorname{sn}^2 \left[ \gamma z \sqrt{3f_1(f_2 - f_3)}, m \right]} \quad (16)$$

where sn is a Jacobian Elliptic function and the squared modulus

$$m^2 = \frac{f_2(f_1 - f_3)}{f_1(f_2 - f_3)}, \quad (17)$$

It is possible to achieve complete power conversion from the pumps to the signal and idler. In this case the power of the idler equals the initial power of the pumps, thus  $F = P_p$ . When inserted into the Hamiltonian, knowing that the value of the Hamiltonian is zero, one see that the requirement of complete power conversion is that  $\delta = 2P_p$ , giving a wave-number mismatch of

$$\Delta\beta = \gamma P_s. \quad (18)$$

This differs significantly from the usually desired value of  $-2\gamma P_p$  which results in the initially fastest growing signal. From Eq. (2), the initial growth rate for  $\Delta\beta = -2\gamma P_p$  is  $G(z) = 1 + \sinh^2 [2\gamma P_p z]$ , whereas the growth rate for  $\Delta\beta = \gamma P_s$  is  $G(z) \approx 1 + \frac{4}{3} \sinh^2 [\sqrt{3}\gamma P_p z]$ . With  $\Delta\beta = \gamma P_s$  the roots of Eq. (9) are  $f_1 = f_2 = P_p$  and  $f_3 = -4P_s/3$ . In this case,  $m = 1$ , reducing the Jacobian Elliptic Function, sn, to hyperbolic tangens functions, tanh. The solution is thus rewritten as

$$F(z) = \frac{4P_p P_s \sinh^2 [\gamma z \sqrt{P_p(3P_p + 4P_s)}]}{3P_p + 4P_s + 4P_s \sinh^2 [\gamma z \sqrt{P_p(3P_p + 4P_s)}}. \quad (19)$$

In the interval  $-6\gamma P_p < \Delta\beta < 2\gamma P_p$ , in which  $g$  is a real parameter, approximate solutions to the roots of Eq. (14) is found by treating  $P_s$  as a small perturbation to the potential equation. Doing this result in three non-zero roots,

$$r_a = -16P_s \frac{P_p^2}{\left(P_p + \frac{1}{6} \frac{\Delta\beta}{\gamma}\right) \left(P_p - \frac{1}{2} \frac{\Delta\beta}{\gamma}\right)} \quad (20)$$

$$r_b = P_p + \frac{1}{6} \frac{\Delta\beta}{\gamma} - 12P_s \frac{P_s - \frac{\Delta\beta}{\gamma}}{2P_p - \frac{\Delta\beta}{\gamma}} \quad (21)$$

$$r_c = P_p - \frac{1}{2} \frac{\Delta\beta}{\gamma} - 4P_s \frac{3P_p + 2\frac{\Delta\beta}{\gamma}}{6P_p + \frac{\Delta\beta}{\gamma}}. \quad (22)$$

The first root,  $r_a$  is the lowest root, thus it is equivalent to  $f_3$ , and it is seen that this root is proportional to  $-P_s$ . The other two roots are equivalent to  $f_1$  and  $f_2$ , however as  $r_b$  is not always greater than  $r_c$ , it will depend on the values of  $\Delta\beta$ , which root is equivalent to which  $f$ . However, the important thing is to see that they are both proportional to  $P_p$ . Therefore, under the assumption that  $P_p \gg P_s$ ,  $m \approx 1$ , the elliptic function sn can be approximated with tanh for small values of  $z$ . Thus, the solution can be expressed as

$$F(z) \approx \frac{\frac{-f_2 f_3}{f_2 - f_3} \sinh^2 [\gamma z \sqrt{3f_1(f_2 - f_3)}]}{1 + \frac{1}{f_2} \frac{-f_2 f_3}{f_2 - f_3} \sinh^2 [\gamma z \sqrt{3f_1(f_2 - f_3)}}}. \quad (23)$$

For very small values of  $z$ , the second term in the denominator can be neglected, reducing it to an expression similar to Eq. (3) Consequently, we may apply the relations:

$$\sqrt{3f_1(f_2 - f_3)} \approx \frac{g}{\gamma} \quad (24)$$

$$-\frac{f_2 f_3}{f_2 - f_3} \approx P_s \left(\frac{2\gamma P_p}{g}\right)^2, \quad (25)$$

which for the interval  $-4\gamma P_p < \Delta\beta < \gamma P_p$ , have a relative error of less than 1% for  $P_s = 0$  dBm, and this error decrease with decreasing input power. With this  $F$  may be expressed as

$$F(z) \approx \frac{F_{QL}(z)}{1 + \frac{F_{QL}(z)}{P_{sat}}} = P_s \frac{\left[ \frac{2\gamma P_p}{g} \sinh^2 [gz] \right]^2}{1 + \frac{P_s}{P_{sat}} \left[ \frac{2\gamma P_p}{g} \sinh^2 [gz] \right]^2} \quad (26)$$

where  $g^2 = (2\gamma P_p)^2 - (\kappa/2)^2$ ,  $\kappa = 2\gamma P_p + \Delta\beta$ , and

$$P_{sat} = f_2 \approx \begin{cases} \frac{1}{6} \left( \frac{\Delta\beta}{\gamma} - P_s \right) + P_p, & -6P_p < \frac{\Delta\beta}{\gamma} < P_s \\ -\frac{1}{2} \left( \frac{\Delta\beta}{\gamma} - P_s \right) + P_p, & P_s < \frac{\Delta\beta}{\gamma} < 2P_p \end{cases} \quad (27)$$

This final expression for  $F$  is a simple expression, using the quasi-linearized result to create an expression that includes the saturation of the pumps.  $P_{sat}$  is the upper limit of the power that can be coupled into the idler. From this it is also clear that using a linear phase mismatch that equals the nonlinear phase shift per unit length of the signal,  $\gamma P_s$ , enables complete power transfer from the pumps into the signal and idler, while when using a linear phase mismatch identical to the nonlinear phase shift of the pump i.e.  $\Delta\beta = -2\gamma P_p$  only can convert about 67%. However, in the latter case when  $\Delta\beta = -2\gamma P_p$  the initial coupling efficiency is higher.

If the two pumps have different power called  $P_a$  and  $P_b$ , where  $P_a > P_b$ , then all that is necessary to change is to replace  $(P_p - F)^2$  with  $(P_a - F)(P_b - F)$  in Eq. (14), and  $2P_p$  with  $P_a + P_b$  in Eq. (10). When this is done, the solution is the same as Eq. (16). Because of the different pump powers, the phase mismatch resulting in full power transfer from the smallest pump is  $\Delta\beta = \gamma P_s + \gamma(P_a - P_b)$ , whereas the fastest growing gain is when  $\Delta\beta = -\gamma(P_a + P_b)$ .

### 3. Discussion

How well Eq. (26) describes the evolution of the idler, compared to Eq. (2) is shown in Fig. 1. From the figure it is seen that the new expression fits well until the power begins to couple back into the pump. In all cases the new approximate expression has a better correlation with the analytic solution than the conventional quasi-linear result in Eq. (2).

Fig. 2 shows the gain for different input powers. The gain has been evaluated by using Eqs. (2), (23) and (26) and it also shows that the new approximation, Eq. (26), is a better approximation to Eq. (23) than the usual approximation, Eq. (2). The new approximation takes the saturation into account, but since it does not include back coupling, it is only useful until back coupling becomes significant. Before the system is in depletion, the gain is symmetric around  $\kappa = 0$  as predicted by Eq. (2), but when saturation set in, the gain profile becomes asymmetric which the new approximation also takes into account. If a setup is constructed with two pumps placed symmetric around the ZDW, then it is possible to obtain a flat gain spectrum over a range of wavelengths, with very high signal gain. The phase mismatch is estimated by Taylor expanding all the propagation constants around the ZDW. Because of the chosen pump symmetry, all  $\beta_n = d^n \beta(\omega) / d\omega^n |_{\omega_{ZD}}$ , where  $n$  is odd, will cancel out, and since  $\beta_2$  is zero at the ZDW, the first term that has influence is  $\beta_4$  which for this setup is  $8.8197 \times 10^{-56} \text{ s}^4/\text{m}$ . The phase mismatch is thus approximated as

$$\Delta\beta = \frac{\beta_4}{12} [(\omega_s - \omega_{ZD})^4 - (\omega_p - \omega_{ZD})^4] \quad (28)$$

When using symmetrically placed pumps and the value of  $\beta_4$  is positive [19], it is very difficult to obtain  $\Delta\beta = -2\gamma P_p$ , unless the pumps are placed very far from the ZDW, however  $\Delta\beta$  is close to zero for a large range, resulting in a high possible power transfer in this region. Fig. 3

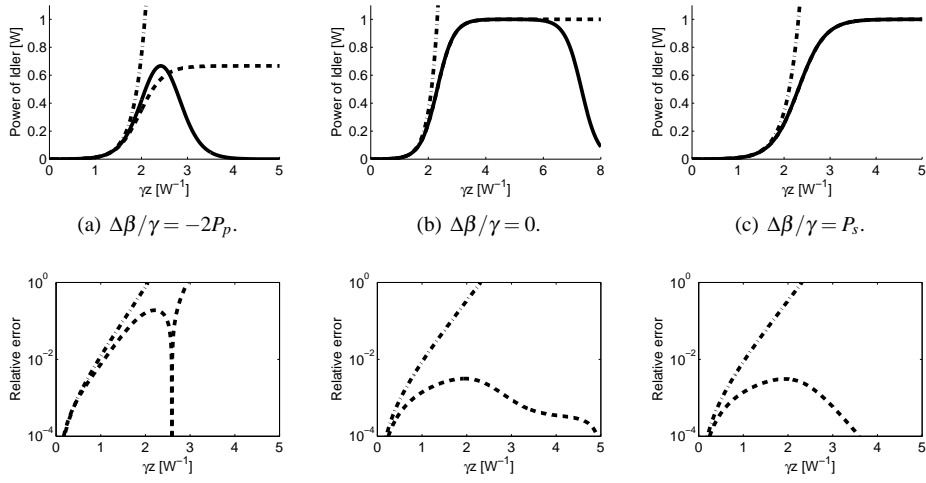


Fig. 1. Evolution of the power of the idler with  $P_p = 30$  dBm and  $P_s = 0$  dBm. The solid line shows the full analytic solution, the dash-dotted is the usual quasi-linearized solution while the dashed is the approximate solution found in this paper. It is evident that the setup in (c) results in complete power transfer while the usual desired setup (a) results in the fastest growing idler. (b) shows that a zero wave-number mismatch results in almost complete power transfer.

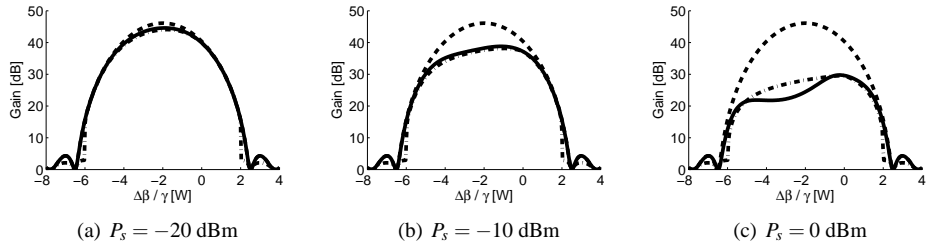
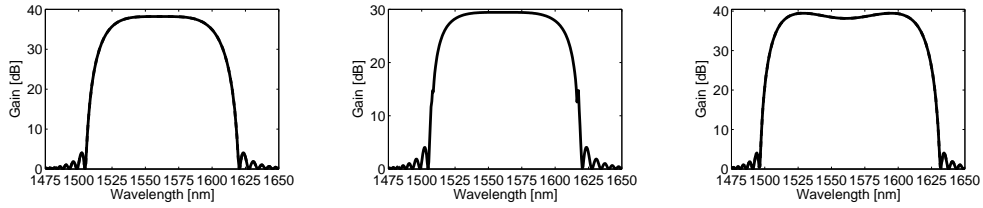


Fig. 2. Gain calculated at  $\gamma L = 3$   $\text{W}^{-1}$  with  $P_p = 30$  dBm. The solid line is the analytically calculated gain, the dashed line is the gain calculated with Eq. (2) while the dash-dotted line is calculated with the approximation found in this paper. In (a) the pumps are not in saturation, thus there is no significant difference between them. However in (b) the pumps begin to be in saturation, which Eq. (2) does not take into account. In (c) the input power is so high that the pumps have depleted and for some values of  $\Delta\beta/\gamma$  the power has started to couple back into the pumps resulting in a lower gain, only the full analytic solution accounts for this phenomenon.

shows gain profiles for a fiber with  $L = 250$  m,  $\lambda_{\text{ZDW}} = 1560.5$  nm, and  $\gamma = 11.5$   $\text{W}^{-1}\text{km}^{-1}$  calculated with Eq. (26).

Because the pumps are placed symmetric around the ZDW, it is, as seen in Fig. 3, possible to achieve a high and flat gain over a broad spectrum. Even if the symmetry is slightly broken, the gain remains reasonably flat, and even increase the spectrum. If Eq. (1) is solved numerically and including loss of 0.74 dB/km, the same spectrum is achieved, only the gain is 1.5 to 2 dB lower.



(a) Symmetrically placed pumps with  $\lambda_p = 1564$  nm and 1557 nm. The signal power is -20 dBm, thus the pumps are undepleted. (b) Symmetrically placed pumps with  $\lambda_p = 1568$  nm and 1553 nm. the signal power is 0 dBm, thus resulting in depleted pumps. (c) Asymmetrically placed pumps with  $\lambda_p = 1564$  nm and 1558 nm and a signal power of -20 dBm.

Fig. 3. Gain profiles for a case with 30 dBm pumps. With symmetrically placed pumps, the gain is very flat over a large bandwidth whereas with slightly asymmetrically placed pumps, the gain is a little less flat, but the spectrum becomes wider.

#### 4. Conclusion

We have shown the exact solution of a dual pumped FOPA as well as a simple yet very useful approximation to the solution which includes pump depletion. With the dual pumped scheme it is possible to obtain a very flat gain over a wide bandwidth. With symmetrically placed pumps, Fig. 3(a), the width of the gain, within 3 dB of max, is 87 nm, in the case of asymmetrically placed pumps, Fig. 3(c), the width is increased to 113 nm. The bandwidth may be further broadened by using slightly asymmetrically placed pumps. However this is only obtainable at the expense of a less flat gain.

We have also shown that although the gain is increasing more rapid as a function of fiber length when  $\Delta\beta = -2\gamma P_p$ , then this phase mismatch will not result in a complete power conversion as is the case when  $\Delta\beta = \gamma P_s$ .

Acknowledgements: EOARD for financial support, grant #XXX

# Draft: Geometric Interpretation of Four Wave Mixing

J. R. Ott,\* H. Steffensen, and K. Rottwitt  
*Technical University of Denmark,  
Department of Photonics Engineering Fotonik-DTU,  
Kgs. Lyngby, DK-2800*

C. J. McKinstrie†  
*Bell Laboratories, Alcatel-Lucent, Holmdel, NJ 07733*

G. G. Luther  
*Engineering Sciences and Applied Mathematics Department,  
McCormick School of Engineering and Applied Sciences,  
Northwestern University, 2145 Sheridan Road, Evanston, IL 60208-3125*

We consider the phenomenon of four-wave mixing. The evolution is analyzed using a variable transform, making it possible to visualize the power and phase information simultaneously. A method of evaluating the dynamics of the system graphically without use of complicated calculations is then proposed. The current version is a draft and therefore contain most calculations.

## I. INTRODUCTION

The optical parametric process of four-wave mixing (FWM) is currently used for several optical communication schemes such as amplification, signal copying, phase conjugation, sampling and regeneration [1, 2].

The governing equations and their evolution given by solutions to elliptic integrals are at this point well known [3, 4], but the usual methods to evaluate power and phase can seem complicated. A recent analysis used the assumption of strong pumps to visualize a specific scheme by the use of a coordinate transform to Stokes-like variables [5] following a routine which has previously been used to describe the evolution of polarization [6].

In the current work we propose an easy way of visualizing the field amplitudes and relative phase of the full nonlinear problem simultaneously as dynamics on a closed 2 dimensional surface in a 3 dimensional space. Using the method proposed, the dynamics is found without having to evaluate any pesky integrals nor differential equations, but simply plotting two implicit equations and and observe their intersection. A similar approach has been used previously for three wave mixing in quadratic nonlinear media [7]. This showed a geometric interpretation of the phenomenon and gave a simple method of visualizing quasi-phase matching used in parametric amplification with quadratic materials.

The following analysis will start by introducing the governing equations for FWM in section II. Furthermore this section review the structure of the Hamiltonian and the use of Poisson bracket formalism for equating governing equations. Section III introduce the geometric representation of the FWM equations using Stokes vectors and the Hamiltonian in this new space is found and the governing equations for the FWM in Stokes space are solved. In section IV the geometric representation is used to evaluate the dynamics of some optical communication schemes showing the advantages of the proposed method.

## II. THE FOUR-WAVE EQUATIONS AND THEIR SYMMETRIES

In the following section the four-wave phenomenon is shortly reviewed along with the Hamiltonian and the use of the Poisson bracket formalism with the Hamiltonian. The well known governing equations for the non-degenerate

---

\*Electronic address: johan.raunkjaerott@fotonik.dtu.dk

†Electronic address: mckinstrie@alcatel-lucent.com

FWM process are [8]

$$\frac{dA_1}{dz} = i\gamma_K[|A_1|^2 + 2(|A_2|^2 + |A_3|^2 + |A_4|^2)]A_1 + 2i\gamma_K A_2 A_3 A_4^* e^{-i\Delta\beta z}, \quad (1a)$$

$$\frac{dA_2}{dz} = i\gamma_K[|A_2|^2 + 2(|A_1|^2 + |A_3|^2 + |A_4|^2)]A_2 + 2i\gamma_K A_1 A_3^* A_4 e^{i\Delta\beta z}, \quad (1b)$$

$$\frac{dA_3}{dz} = i\gamma_K[|A_3|^2 + 2(|A_1|^2 + |A_2|^2 + |A_4|^2)]A_3 + 2i\gamma_K A_1 A_2^* A_4 e^{i\Delta\beta z}, \quad (1c)$$

$$\frac{dA_4}{dz} = i\gamma_K[|A_4|^2 + 2(|A_1|^2 + |A_2|^2 + |A_3|^2)]A_4 + 2i\gamma_K A_1^* A_2 A_3 e^{-i\Delta\beta z}. \quad (1d)$$

These are obtained by a slowly varying amplitude approximation of Maxwell's equations for resonant interaction of four lightwaves propagating in a centrosymmetric material.  $A_j$  is the slowly varying complex field envelopes for the  $j$ 'th field,  $\gamma_K$  is the nonlinear Kerr coefficient assumed to be frequency independent, and  $\Delta\beta = \beta_1 - \beta_2 - \beta_3 + \beta_4$  is the wavenumber mismatch with the wavenumber of the  $j$ 'th field being  $\beta_j = \beta(\omega_j)$ . The numbering is either from high to low frequency or from low to high. The waves 1 and 4 are thus the side bands while 2 and 3 denote the inner bands.

By inspection, the set of Eqns. (1) has the Hamiltonian

$$\tilde{H} = \gamma_K \sum_{n=1}^4 \sum_{m=1}^4 d_{n,m} |A_n|^2 |A_m|^2 + 2\gamma_K (A_1^* A_2 A_3 A_4^* e^{-i\Delta\beta z} + A_1 A_2^* A_3^* A_4 e^{i\Delta\beta z}), \quad (2)$$

with  $d_{n,n} = \frac{1}{2}$  and  $d_{n,m} = 1$  when  $n \neq m$ .

Making use of the conservation of power  $P_t = \sum_{n=1}^4 |A_n|^2$  and introducing the change of variables  $\xi = \gamma_K P_t z$  and the rescaled rotating frame

$$A_j = q_j \sqrt{P_t} e^{-i\beta_j z + 2i\gamma_K P_t z} \quad (3)$$

the four-wave equations become

$$\frac{dq_1}{d\xi} = i\Gamma_1 q_1 - i|q_1|^2 q_1 + 2iq_2 q_3 q_4^*, \quad (4a)$$

$$\frac{dq_2}{d\xi} = i\Gamma_2 q_2 - i|q_2|^2 q_2 + 2iq_1 q_3^* q_4, \quad (4b)$$

$$\frac{dq_3}{d\xi} = i\Gamma_3 q_3 - i|q_3|^2 q_3 + 2iq_1 q_2^* q_4, \quad (4c)$$

$$\frac{dq_4}{d\xi} = i\Gamma_4 q_4 - i|q_4|^2 q_4 + 2iq_1^* q_2 q_3, \quad (4d)$$

with  $\Gamma_j = \frac{\beta_j}{\gamma_K P_t}$  being the rescaled wavenumber.

The Hamiltonian for these normalized fields is

$$H = \sum_{n=1}^4 \Gamma_n |q_n|^2 - \frac{1}{2} \sum_{n=1}^4 |q_n|^4 + 2(q_1^* q_2 q_3 q_4^* + q_1 q_2^* q_3^* q_4). \quad (5)$$

Thereby the equations have the canonical Hamiltonian structure

$$\frac{dq_j}{dz} = i\{q_j, H\} = i\frac{\partial H}{\partial q_j^*}, \quad (6)$$

with the Poisson bracket defined as [9]

$$\{P, Q\}_{q_\alpha, q_\alpha^*} = \sum_{\alpha} \left( \frac{\partial P}{\partial q_\alpha} \frac{\partial Q}{\partial q_\alpha^*} - \frac{\partial P}{\partial q_\alpha^*} \frac{\partial Q}{\partial q_\alpha} \right), \quad (7)$$

with  $\{P, P\} = 0$  and  $\{P, Q\} = -\{Q, P\}$ , which is the classical counterpart to the quantum mechanical commutator. The index  $q_\alpha, q_\alpha^*$  denote the choice of canonical variables for the Poisson bracket and will be omitted in the following.

Due to the normalization, Eq. (3), the Hamiltonian no longer explicitly depend on the propagation parameter, it is a constant of motion. Furthermore the governing equations have the conserved quantities

$$K_1 = |q_1|^2 - |q_4|^2, \quad (8a)$$

$$K_2 = |q_2|^2 - |q_3|^2, \quad (8b)$$

$$K_3 = |q_1|^2 + |q_2|^2, \quad (8c)$$

$$K_4 = |q_3|^2 + |q_4|^2, \quad (8d)$$

$$P = |q_1|^2 + |q_2|^2 + |q_3|^2 + |q_4|^2, \quad (8e)$$

also known as the Manley-Rowe relations (MRR)s [10, 11]. The physical significance of these can most easily be understood by a quantum mechanical interpretation as follows. The first two of the relations signify that in the inner and outer bands, photons are created or annihilated in pairs. The third and fourth relation signify that creating the photon pairs in the inner or outer bands annihilates photon pairs in the outer or inner bands. Using the first two relations either of the fields in the third and fourth relation can be interchanged with its field pair partner, i.e.  $K_3 - K_1 = |q_4|^2 + |q_2|^2$  which is the same as interchanging 1 and 4. The last of the relations signify conservation of photons and due to the rescaling of the fields  $P = 1$ . The MRRs are seen to be a overfull set so that only three of them are independent.

Furthermore the Hamiltonian, and thus the governing equations for the fields, is seen only to depend on the phase difference  $\Delta\phi = \phi_2 + \phi_3 - \phi_1 - \phi_4$ , where the phase is defined by  $q_j(\xi) = |q_j(\xi)|e^{i\phi_j(\xi)}$ . Therefore the eight coupled real nonlinear differential equations governing FWM can be reduced to four equations governing the real amplitudes and one governing equation for the phase difference. This can be reduced to a single potential equation for either of the amplitudes which is solvable using elliptic integrals. Subsequently all the other amplitudes and the phase difference can be calculated [3, 4]. In the following the problem will be solved in another way giving a geometric interpretation of all the powers and the phase difference simultaneously. The current solution method also include the common one as a special case.

As stated by Noether's Theorem the four invariant MRRs correspond to four symmetries of the governing equations, Eqs. (4). These symmetries are the Gauge invariances

$$(q_1, q_2, q_3, q_4) \rightarrow (q_1 e^{-i\phi_1}, q_2, q_3, q_4 e^{i\phi_1}), \quad (9a)$$

$$(q_1, q_2, q_3, q_4) \rightarrow (q_1, q_2 e^{-i\phi_2}, q_3 e^{i\phi_2}, q_4), \quad (9b)$$

$$(q_1, q_2, q_3, q_4) \rightarrow (q_1 e^{-i\phi_3}, q_2 e^{-i\phi_3}, q_3, q_4), \quad (9c)$$

$$(q_1, q_2, q_3, q_4) \rightarrow (q_1, q_2, q_3 e^{-i\phi_4}, q_4 e^{-i\phi_4}). \quad (9d)$$

This is seen by letting either of the MRRs act as the Hamiltonian in Eq. (6) and determining the effect of the evolution, i.e. calculating  $\frac{dq_j}{d\xi} = \{q_j, K_k\}$ . E.g. for  $K_1$  this would result in

$$\frac{dq_1}{d\xi} = i\{q_1, K_1\} = i\frac{dK_1}{dq_1^*} = iq_1, \quad (10a)$$

$$\frac{dq_2}{d\xi} = i\{q_2, K_1\} = i\frac{dK_1}{dq_2^*} = 0, \quad (10b)$$

$$\frac{dq_3}{d\xi} = i\{q_3, K_1\} = i\frac{dK_1}{dq_3^*} = 0, \quad (10c)$$

$$\frac{dq_4}{d\xi} = i\{q_4, K_1\} = i\frac{dK_1}{dq_4^*} = iq_4, \quad (10d)$$

i.e. an equal, but opposite, phase shift of  $q_1$  and  $q_4$  which corresponds to the Gauge invariance Eq. (9a).

It is easy to show that the four-wave equations, Eqs. (4), are invariant under the Gauge transforms, Eqs. (9).

### III. REDUCTION TO FOUR-WAVE SURFACES

In this section the dynamics of the four-wave equations will be reduced to dynamics on a closed surface in a 3 dimensional space. A simple example of previous use of such reduction is that of projection of polarization onto the Poincaré sphere. In that case the reduction of dimension is performed by using a set of invariant coordinates

with respect to the phase symmetry of the polarization, the Stokes parameters, that project the dynamics onto the Poincaré sphere. Similar in our case a set of Stokes-like parameters which are invariant under the same Gauge transforms must be chosen. Such a set of real parameters  $X$ ,  $Y$  and  $Z$  could thus be chosen as

$$X + iY = q_1^* q_2 q_3 q_4^*, \quad (11a)$$

$$Z = \sum_{n=1}^4 p_n |q_n|^2, \quad (11b)$$

with  $p_n$  being some constants that can be chosen freely to focus an analysis on specific properties. Choices of the  $p_j$ 's will be further investigated shortly.

By taking the square modulus of  $X + iY$  and expressing the  $|q_j|^2$ 's in terms of the  $Z$ -coordinate and the MRRs one obtain the expression

$$X^2 + Y^2 = |q_1|^2 |q_2|^2 |q_3|^2 |q_4|^2 = \kappa^4 (Z - Z_1)(Z + Z_2)(Z + Z_3)(Z - Z_4), \quad (12)$$

with  $\kappa = (p_1 - p_2 - p_3 + p_4)^{-1}$  and

$$Z_1 = p_2 K_3 + p_3 (K_1 + K_4) - p_4 K_1, \quad (13a)$$

$$Z_2 = -p_1 K_3 + p_3 K_2 - p_4 (K_2 + K_4), \quad (13b)$$

$$Z_3 = -p_1 (K_1 + K_4) - p_2 K_2 - p_4 K_4, \quad (13c)$$

$$Z_4 = p_1 K_1 + p_2 (K_2 + K_4) + p_3 K_4. \quad (13d)$$

The constants  $Z_j$ 's can be written in matrix notation as

$$\begin{pmatrix} Z_1 \\ Z_2 \\ Z_3 \\ Z_4 \end{pmatrix} = \begin{pmatrix} 0 & K_3 & K_1 + K_4 & -K_1 \\ -K_3 & 0 & K_2 & -(K_2 + K_4) \\ -(K_1 + K_4) & -K_2 & 0 & -K_4 \\ K_1 & K_2 + K_4 & K_4 & 0 \end{pmatrix} \begin{pmatrix} p_1 \\ p_2 \\ p_3 \\ p_4 \end{pmatrix} \quad (14)$$

from which it is seen that the choice of signs for the  $Z_j$ 's in Eq. (12), ensure a symmetric matrix.

The coefficients  $Z_j$  can be found by inserting the MRR in  $Z$  leaving only  $|q_j|^2$  which can then be isolated, i.e. for  $Z_1$

$$\begin{aligned} Z &= p_1 |q_1|^2 + p_2 |q_2|^2 + p_3 |q_3|^2 + p_4 |q_4|^2 \\ &= p_1 |q_1|^2 + p_2 (K_3 - |q_1|^2) + p_3 (K_1 + K_4 - |q_1|^2) + p_4 (|q_1|^2 - K_1) \\ &= (p_1 - p_2 - p_3 + p_4) |q_1|^2 + p_2 K_2 + p_3 (K_1 + K_4) - p_4 K_1 \\ &= \kappa^{-1} |q_1|^2 + Z_1, \end{aligned} \quad (15)$$

while for  $Z_2$

$$\begin{aligned} Z &= p_1 |q_1|^2 + p_2 |q_2|^2 + p_3 |q_3|^2 + p_4 |q_4|^2 \\ &= p_1 (K_3 - |q_2|^2) + p_2 |q_2|^2 + p_3 (-K_2 + |q_2|^2) + p_4 (K_1 + K_4 - |q_2|^2) \\ &= (p_1 - p_2 - p_3 + p_4) |q_1|^2 + p_1 K_2 - p_3 K_2 + p_4 (K_1 + K_4) \\ &= -\kappa^{-1} |q_2|^2 - Z_2. \end{aligned} \quad (16)$$

By defining

$$\phi = X^2 + Y^2 - \kappa^4 (Z - Z_1)(Z + Z_2)(Z + Z_3)(Z - Z_4) \quad (17)$$

we immediately acquire the implicit equation,  $\phi = 0$ , from Eq. (12), which yield the four-wave surface in  $(X, Y, Z)$  space. This surface restricts the evolution of the fields and phase to a two dimensional surface in a three dimensional space. This space describe the relative phase of the fields through the  $X$  and  $Y$  coordinates and specific field intensities through  $Z$ , specified by the choice of the  $p_j$  parameters. Choosing  $p_j = 1$  while  $p_{n \neq j} = 0$  yield the evolution of the  $j$ 'th field intensity giving the exact same result as the usual analysis. Choosing instead  $p_1 = p_4 = 1$  or  $p_2 = p_3 = 1$  yield the evolution of the either the side bands or the inner bands intensities while choosing  $p_1 = p_4 = 1 = -p_2 = -p_3$  investigate the transfer of energy between the inner bands and the side bands.

The Hamiltonian in terms of the  $(X, Y, Z)$  coordinates is given by

$$\begin{aligned}
H &= \kappa [\Gamma_1(Z - Z_1) - \Gamma_2(Z + Z_2) - \Gamma_3(Z + Z_3) + \Gamma_4(Z - Z_4)] \\
&\quad - \frac{\kappa^2}{2} [(Z - Z_1)^2 + (Z + Z_2)^2 + (Z + Z_3)^2 + (Z - Z_4)^2] + 4X \\
&= \kappa \Delta \Gamma Z - \kappa (\Gamma_1 Z_1 + \Gamma_2 Z_2 + \Gamma_3 Z_3 + \Gamma_4 Z_4) \\
&\quad - \frac{\kappa^2}{2} [4Z^2 - 2(Z_1 - Z_2 - Z_3 + Z_4)Z + Z_1^2 + Z_2^2 + Z_3^2 + Z_4^2] + 4X \\
&= -2\kappa^2 Z^2 + \kappa [\Delta \Gamma + \kappa(Z_1 - Z_2 - Z_3 + Z_4)] Z \\
&\quad - \kappa \left[ \Gamma_1 Z_1 + \Gamma_2 Z_2 + \Gamma_3 Z_3 + \Gamma_4 Z_4 + \frac{\kappa}{2} (Z_1^2 + Z_2^2 + Z_3^2 + Z_4^2) \right] + 4X \\
&= -2\kappa^2 Z^2 + \kappa \Omega Z - \Pi + 4X
\end{aligned} \tag{18}$$

which should be noted to be independent of  $Y$ , linear in  $X$  and quadratic in  $Z$ . Here the rescaled wave number mismatch  $\Delta \Gamma = \Gamma_1 - \Gamma_2 - \Gamma_3 + \Gamma_4 = \frac{\Delta \beta}{\gamma \kappa P_i}$ , the phase mismatch  $\Omega = \Delta \Gamma + \kappa(Z_1 - Z_2 - Z_3 + Z_4)$  and  $\Pi = \kappa [\Gamma_1 Z_1 + \Gamma_2 Z_2 + \Gamma_3 Z_3 + \Gamma_4 Z_4 + \frac{\kappa}{2} (Z_1^2 + Z_2^2 + Z_3^2 + Z_4^2)]$  has been defined for convenience. The dynamics of the variables  $(X, Y, Z)$  lie on the orbits formed by the intersection of the Hamiltonian with the surface,  $\phi = 0$ .

The evolution of the four-wave equations can of course be solved analytically in the new coordinate system which will be done in the following. Any readers who are not interested in rigorous math can though with great benefit skip this and go to section IV.

The Poisson bracket relations for the new variables are

$$\begin{aligned}
\{Y, X\} &= \sum_{n=1}^4 \left( \frac{\partial Y}{\partial q_n} \frac{\partial X}{\partial q_n^*} - \frac{\partial Y}{\partial q_n^*} \frac{\partial X}{\partial q_n} \right) \\
&= \frac{i}{4} \sum_{n=1}^4 \left( \frac{\partial q_1^* q_2 q_3 q_4^* + q_1 q_2^* q_3^* q_4}{\partial q_n} \frac{\partial q_1^* q_2 q_3 q_4^* - q_1 q_2^* q_3^* q_4}{\partial q_n^*} \right. \\
&\quad \left. - \frac{\partial q_1^* q_2 q_3 q_4^* + q_1 q_2^* q_3^* q_4}{\partial q_n^*} \frac{\partial q_1^* q_2 q_3 q_4^* - q_1 q_2^* q_3^* q_4}{\partial q_n} \right) \\
&= \frac{i}{2} (|q_2|^2 |q_3|^2 |q_4|^2 - |q_1|^2 |q_3|^2 |q_4|^2 - |q_1|^2 |q_2|^2 |q_4|^2 + |q_1|^2 |q_2|^2 |q_3|^2) \\
&= \frac{\kappa^3 i}{2} \left[ (Z + Z_2)(Z + Z_3)(Z - Z_4) + (Z - Z_1)(Z + Z_3)(Z - Z_4) \right. \\
&\quad \left. + (Z - Z_1)(Z + Z_2)(Z - Z_4) + (Z - Z_1)(Z + Z_2)(Z + Z_3) \right] \\
&= -\frac{i}{2\kappa} \frac{\partial \phi}{\partial Z},
\end{aligned} \tag{19a}$$

$$\begin{aligned}
\{X, Z\} &= \frac{1}{2} (p_1 - p_2 - p_3 + p_4) (q_1^* q_2 q_3 q_4^* - q_1 q_2^* q_3^* q_4) \\
&= -i\kappa^{-1} Y,
\end{aligned} \tag{19b}$$

$$\begin{aligned}
\{Y, Z\} &= -\frac{1}{2i} (p_1 - p_2 - p_3 + p_4) (q_1^* q_2 q_3 q_4^* + q_1 q_2^* q_3^* q_4) \\
&= i\kappa^{-1} X,
\end{aligned}$$

$$\begin{aligned}
\{X, Z^2\} &= \sum_{n=1}^4 \left( \frac{\partial X}{\partial q_n} \frac{\partial Z^2}{\partial q_n^*} - \frac{\partial X}{\partial q_n^*} \frac{\partial Z^2}{\partial q_n} \right) \\
&= 2Z \sum_{n=1}^4 \left( \frac{\partial X}{\partial q_n} \frac{\partial Z}{\partial q_n^*} - \frac{\partial X}{\partial q_n^*} \frac{\partial Z}{\partial q_n} \right) \\
&= 2Z \{X, Z\}.
\end{aligned} \tag{19c}$$

Using these the dynamical equations for the  $(X, Y, Z)$  coordinates are

$$\begin{aligned}\frac{dX}{d\xi} &= i\{X, H\} \\ &= -2\kappa^2 i\{X, Z^2\} + \kappa\Omega i\{X, Z\} - i\{X, \Pi\} + 4i\{X, X\} \\ &= -2\kappa^2 i(-2iZ\kappa^{-1}Y) + \kappa\Omega i(-i\kappa^{-1}Y) - 0 + 0 \\ &= -(4\kappa Z - \Omega)Y,\end{aligned}\tag{20a}$$

$$\begin{aligned}\frac{dY}{d\xi} &= -2\kappa^2 i\{Y, Z^2\} + \kappa\Omega i\{Y, Z\} - i\{Y, \Pi\} + 4i\{Y, X\} \\ &= -2\kappa^2 i(2iZ\kappa^{-1}X) + \kappa\Omega i(i\kappa^{-1}X) - 0 + 4i\left(-\frac{i}{2\kappa}\frac{\partial\phi}{\partial Z}\right) \\ &= (4\kappa Z - \Omega)X + 2\frac{\partial\phi}{\partial Z},\end{aligned}\tag{20b}$$

$$\begin{aligned}\frac{dZ}{d\xi} &= -2\kappa^2 i\{Z, Z^2\} + \kappa\Omega i\{Z, Z\} - i\{Z, \Pi\} + 4i\{Z, X\} \\ &= -0 + 0 - 0 + 4i(i\kappa^{-1}Y) \\ &= -4\kappa^{-1}Y.\end{aligned}\tag{20c}$$

In this form the coupling between  $X$  and  $Y$ , i.e. the evolution of the phase, consist of a contribution equivalent to a harmonic oscillator with frequency  $\Omega$  and a power dependent contribution. This clearly show the relation that the phase of the four-wave interaction is dependent on the power.

Differentiation of the equation for  $Z$ , inserting the equation for  $Y$  and eliminating  $X$  using the conservation of the Hamiltonian  $H$  gives

$$\begin{aligned}\frac{d^2Z}{d\xi^2} &= -4\kappa^{-1}\frac{dY}{d\xi} \\ &= -4\kappa^{-1}\left[(4\kappa Z - \Omega)X + 2\frac{\partial\phi}{\partial Z}\right] \\ &= -\kappa^{-1}(4\kappa Z - \Omega)(H + 2\kappa^2 Z^2 - \kappa\Omega Z + \Pi) - 8\kappa^{-1}\frac{\partial\phi}{\partial Z}\end{aligned}\tag{21}$$

$$\begin{aligned}&= -\kappa^{-1}[8\kappa^3 Z^3 - 6\kappa^2\Omega Z^2 + \kappa(4H + 4\Pi + \Omega^2)Z - \Omega(H + \Pi)] - 8\kappa^{-1}\frac{\partial\phi}{\partial Z} \\ &= -f(Z).\end{aligned}\tag{22}$$

Then, by using the common tricks that

$$2\frac{dZ}{d\xi}\frac{d^2Z}{d\xi^2} = \frac{d}{d\xi}\left(\frac{dZ}{d\xi}\right)^2\tag{23}$$

and that

$$\frac{dZ}{d\xi}g(Z) = \frac{d}{d\xi}\int g(Z)dZ,\tag{24}$$

it is possible to write the equation for  $Z$  as the potential equation

$$\frac{1}{2}\left(\frac{dZ}{d\xi}\right)^2 + U(Z) = E,\tag{25}$$

where

$$U(z) = 2\kappa^2 Z^4 - 2\kappa\Omega Z^3 + 2\left[H + \Pi + \left(\frac{\Omega}{2}\right)^2\right]Z^2 - \frac{\Omega}{\kappa}(H + \Pi) - 8\kappa^{-1}\phi(X = Y = 0, Z),\tag{26}$$

and  $E$  is a constant of integration. The potential is thus a fourth order polynomial and the potential equation can thus be solved using elliptic equations. The equations of  $X$  and  $Y$  can thus be written on the form

$$\frac{d}{d\xi}\begin{pmatrix} X \\ Y \end{pmatrix} = \begin{pmatrix} 0 & -[4\kappa Z(\xi) - \Omega] \\ 4\kappa Z(\xi) - \Omega & 0 \end{pmatrix} \begin{pmatrix} X \\ Y \end{pmatrix} + 2\frac{\partial\phi}{\partial Z}\begin{pmatrix} 0 \\ 1 \end{pmatrix}\tag{27}$$

having a solution on the form

$$\begin{pmatrix} X \\ Y \end{pmatrix} = \begin{pmatrix} X_{\text{hom}} \\ Y_{\text{hom}} \end{pmatrix} + \begin{pmatrix} 0 \\ Y_{\text{inhom}} \end{pmatrix}, \quad (28)$$

where  $X_{\text{hom}}$ ,  $Y_{\text{hom}}$  and  $Y_{\text{inhom}}$  are the solutions to

$$\frac{d}{d\xi} \begin{pmatrix} X_{\text{hom}} \\ Y_{\text{hom}} \end{pmatrix} = \begin{pmatrix} 0 & -g(\xi) \\ g(\xi) & 0 \end{pmatrix}, \quad (29)$$

with

$$g(\xi) = 4\kappa Z(\xi) - \Omega, \quad (30)$$

and

$$\frac{dY_{\text{inhom}}}{d\xi} = 2 \frac{\partial \phi}{\partial Z}. \quad (31)$$

This procedure will produce the evolution in the  $(X, Y, Z)$  coordinates which can be related to the relative phase from the  $X$  and  $Y$  dynamics and the intensities using the specific choice of  $Z$  and the MRRs. The phases of the specific field can then be found by splitting the governing equations for complex fields  $q_j$  into equations for the real amplitude and phases, inserting the solutions for the amplitudes into the equations for the phases and integrating.

This method of calculating the evolution though seem cumbersome and yield the same results as the usual. Another simple method giving an intuitive geometric representation with a minimum of calculations will be described in the next section.

#### IV. THE REDUCED PHASE SPACE

In the last section the four-wave system has been shown to lie on a trajectory in the  $(X, Y, Z)$  space and the method for finding the trajectory was sketched. In this section another way of acquiring knowledge of the dynamics of the system is described.

As shown the four-wave system was restricted to the dynamics on the surface given by  $\phi = 0$ . This surface is determined strictly from the definitions of  $(X, Y, Z)$  and the conserved MRRs and not the physical parameters of the system such as dispersion and nonlinearity and neither the phases of the fields. Using that the Hamiltonian is also a constant of motion, the trajectory of the four-wave system can be found as the intersection between the four-wave surface and the Hamiltonian. The Hamiltonian depends on the dispersion and the phase of the fields.

An example of this could be a single pump parametric amplifier, i.e. the degenerate case at which  $q_2 = q_3$ . By choosing  $p_1 = p_4 = -p_2 = -p_3 = 1$  the transfer of energy is considered since  $Z = -1$  signify that all energy is in the inner band(s),  $q_2$  and  $q_3$ , while  $Z = 1$  signify that all energy is in the outer bands  $q_1$  and  $q_4$ . As an example lets have the initial values  $q_1(0) = \sqrt{\frac{1}{5}}e^{i\pi/2}$ ,  $q_2(0) = q_3(0) = \sqrt{\frac{2}{5}}$  and  $q_4(0) = 0$ , i.e for copying a signal from  $q_1$  to  $q_4$  or the amplification of  $q_1$ . Such initial values yield the four-wave surface shown in Fig. 1(a). The surface is seen to be tear-drop shaped between  $Z_{\text{min}} = -\frac{3}{5}$  and  $Z_{\text{max}} = 1$ . The lower bound show that all power cannot be transferred to the pump which is well known for the case where  $|q_1(0)|^2 \neq |q_4(0)|^2$ . The pointy top of the tear-drop show the full conversion of energy to the sidebands and the non-analytical shape of the surface show that the conversion can only happen in the infinite time limit. In the case where  $|q_1(0)|^2 = |q_4(0)|^2$  and  $|q_2(0)|^2 = |q_3(0)|^2$  the possibility of full conversion both to the side bands and to the inner bands exist, giving two pointy ends of the sphere as shown in Fig. 1(b) with the initial values  $|q_1(0)|^2 = |q_4(0)|^2 = \frac{1}{6}$  and  $|q_2(0)|^2 = |q_3(0)|^2 = \frac{2}{6}$ . If on the other hand  $|q_1(0)|^2 \neq |q_4(0)|^2$  and  $|q_2(0)|^2 \neq |q_3(0)|^2$  it is not possible to have full power transfer and thus the four-wave surface is smooth as shown in Fig. 1(c) for the initial values  $|q_1(0)|^2 = \frac{1}{10}$ ,  $|q_2(0)|^2 = \frac{3}{10}$ ,  $|q_3(0)|^2 = \frac{4}{10}$  and  $|q_4(0)|^2 = \frac{2}{10}$ . The last example could of cause not happen for the degenerate scheme as, per definition,  $q_2 = q_3$  in that case.

Lets get back to the single pump parametric amplifier. In order to determine the evolution on the four-wave surface we only need to calculate the Hamiltonian and observe the intersection with the four-wave surface. For an amplifier setup having the dispersion  $\Gamma_1 = 0.1$ ,  $\Gamma_2 = \Gamma_3 = 0.2$  and  $\Gamma_4 = 0.3$ , i.e. having zero wave-number mismatch,  $\Delta\Gamma = 0$ , the Hamiltonian is shown in Fig. 2(a) and the intersection between the Hamiltonian and the four-wave surface is shown in Fig. 2(b). As seen the zero wave-number mismatch does not yield the full energy transfer as is well known. The full energy transfer is though possible for  $\Delta\Gamma = |q_1(0)|^2 + |q_4(0)|^2$  which is seen by setting  $H_0 = H_{\text{opt}}$  and isolating  $\Delta\Gamma$ , where the index 0 denote the fields at  $\xi = 0$  and opt denote the optimal power transfer, i.e.  $X_{\text{opt}} = 0$  and  $Z_{\text{opt}} = 1$ .

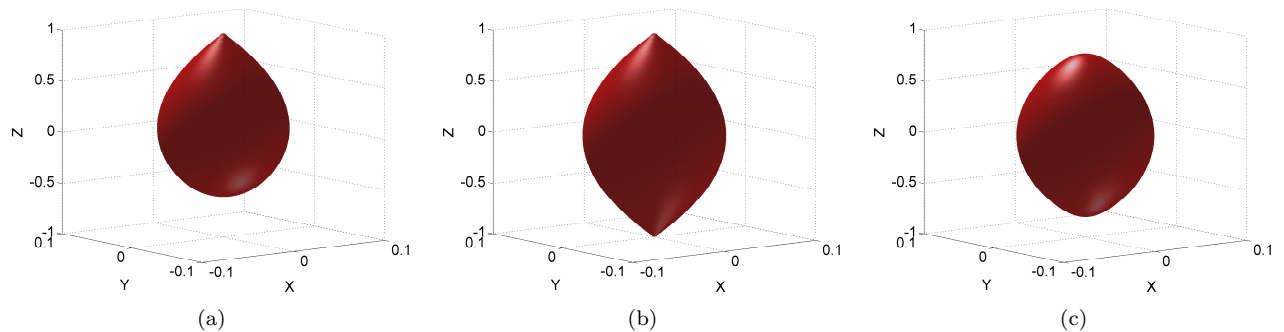


FIG. 1: The four-wave surface with  $p_1 = p_4 = -p_2 = -p_3 = 1$  and the initial values (a)  $|q_1(0)|^2 = \frac{1}{5}$ ,  $|q_2(0)|^2 = |q_3(0)|^2 = \frac{2}{5}$  and  $|q_4(0)|^2 = 0$ , (b)  $|q_1(0)|^2 = |q_4(0)|^2 = \frac{1}{6}$  and  $|q_2(0)|^2 = |q_3(0)|^2 = \frac{2}{6}$ , and (c)  $|q_1(0)|^2 = \frac{1}{10}$ ,  $|q_2(0)|^2 = \frac{3}{10}$ ,  $|q_3(0)|^2 = \frac{4}{10}$  and  $|q_4(0)|^2 = \frac{2}{10}$ .

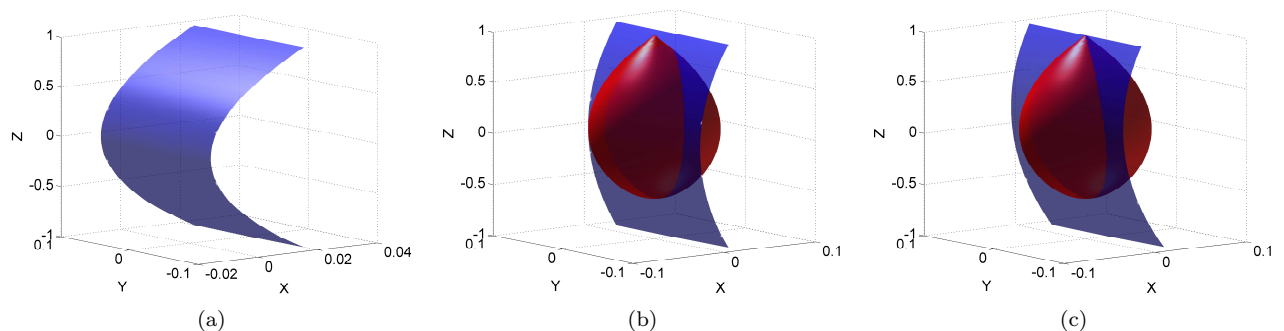


FIG. 2: (a) The four-wave Hamiltonian and (b) the intersection between the four-wave surface and the Hamiltonian. Both with the initial values  $q_1(0) = \sqrt{\frac{1}{5}}e^{i\pi/2}$ ,  $q_2(0) = q_3(0) = \sqrt{\frac{2}{5}}$  and  $q_4(0) = 0$ , while  $p_1 = p_4 = -p_2 = -p_3 = 1$  and  $\Gamma_1 = 0.1$ ,  $\Gamma_2 = \Gamma_3 = 0.2$  and  $\Gamma_4 = 0.3$ . (c) The intersection between the four-wave surface and the Hamiltonian with the initial values  $q_1(0) = \sqrt{\frac{1}{5}}e^{i\pi/2}$ ,  $q_2(0) = q_3(0) = \sqrt{\frac{2}{5}}$  and  $q_4(0) = 0$ , while  $p_1 = p_4 = -p_2 = -p_3 = 1$  and  $\Gamma_1 = 0.1$ ,  $\Gamma_2 = \Gamma_3 = 0.2$  and  $\Gamma_4 = 0.5$  giving  $\Delta\Gamma = 0.2 = |q_1(0)|^2$ .

An example of full energy transfer is shown in Fig. 2(c) with the initial values  $q_1(0) = \sqrt{\frac{1}{5}}e^{i\pi/2}$ ,  $q_2(0) = q_3(0) = \sqrt{\frac{2}{5}}$  and  $q_4(0) = 0$ , while  $p_1 = p_4 = -p_2 = -p_3 = 1$  and  $\Gamma_1 = 0.1$ ,  $\Gamma_2 = \Gamma_3 = 0.2$  and  $\Gamma_4 = 0.5$  giving  $\Delta\Gamma = 0.2 = |q_1(0)|^2$ .

- 
- [1] S. Radic and C. J. McKinstrie, IEICE Trans. Electron. E88C pp. 859–869 (2005).
  - [2] J. Hansryd, P. Andrekson, M. Westlund, J. Li, and P. Hedekvist, IEEE J. Sel. Top. Quantum Electron. **8**, 506 (2002).
  - [3] C. J. McKinstrie and G. G. Luther, Physics Letters A **127**, 14 (1988).
  - [4] G. Cappellini and S. Trillo, J. Opt. Soc. Am. B **8**, 824 (1991).
  - [5] C. J. McKinstrie, Opt. Com. **282**, 1557 (2009).
  - [6] J. P. Gordon and H. Kogelnik, Proc. Natl. Acad. Sci. **97**, 4541 (2000).
  - [7] G. G. Luther, M. S. Alber, J. E. Marsden, and J. M. Robbins, J. Opt. Soc. Am. B **17**, 932 (2000).
  - [8] G. Agrawal, *Nonlinear Fiber Optics* (Academic Press, San Diego, 2007), 4th ed.
  - [9] H. Goldstein, *Classical Mechanics* (Addison-Wesley, New York, 1980), 2nd ed.
  - [10] J. M. Manley and H. E. Rowe, Proc. IRE **44**, 904 (1956).
  - [11] M. T. Weiss, Proc. IRE **45**, 1012 (1957).